Neurotox Res (2017) 32:614–623
DOI 10.1007/s12640-017-9775-0

ORIGINAL ARTICLE

Knockdown of Myo-Inositol Transporter SMIT1 Normalizes Cholinergic and Glutamatergic Function in an Immortalized Cell Line Established from the Cerebral Cortex of a Trisomy 16 Fetal Mouse, an Animal Model of Human Trisomy 21 (Down Syndrome)

Ana María Cárdenas[1] · **Paola Fernández-Olivares**[1,2] · **Ignacio Díaz-Franulic**[1,3,4] · **Arlek M. González-Jamett**[1] · **Takeshi Shimahara**[5] · **Juan Segura-Aguilar**[2] · **Raúl Caviedes**[2] · **Pablo Caviedes**[2]

Received: 25 April 2017 / Revised: 21 June 2017 / Accepted: 28 June 2017 / Published online: 10 July 2017

Abstract The Na^+/myo-inositol cotransporter (SMIT1) is overexpressed in human Down syndrome (DS) and in trisomy 16 fetal mice (Ts16), an animal model of the human condition. SMIT1 overexpression determines increased levels of intracellular myo-inositol, a precursor of phophoinositide synthesis. SMIT1 is overexpressed in CTb cells, an immortalized cell line established from the cerebral cortex of a Ts16 mouse fetus. CTb cells exhibit impaired cytosolic Ca^{2+} signals in response to glutamatergic and cholinergic stimuli (increased amplitude and delayed time-dependent kinetics in the decay post-stimulation), compared to our CNh cell line, derived from the cerebral cortex of a euploid animal. Considering the role of myo-inositol in intracellular signaling, we normalized SMIT1 expression in CTb cells using specific mRNA antisenses. Forty-eight hours post-transfection, SMIT1 levels in CTb cells reached values comparable to those of CNh cells. At this time, decay kinetics of Ca^{2+} signals induced by either glutamate, nicotine, or muscarine were accelerated in transfected CTb cells, to values similar to those of CNh cells. The amplitude of glutamate-induced cytosolic Ca^{2+} signals in CTb cells was also normalized. The results suggest that SMIT1 overexpression contributes to abnormal cholinergic and glutamatergic Ca^{2+} signals in the trisomic condition, and knockdown of DS-related genes in our Ts16-derived cell line could constitute a relevant tool to study DS-related neuronal dysfunction.

Keywords Down syndrome · SMIT1 · Myo-inositol · Calcium · Glutamate · Cholinergic

✉ Pablo Caviedes
pcaviede@med.uchile.cl

[1] Centro Interdisciplinario de Neurociencia de Valparaíso, Facultad de Ciencias, Universidad de Valparaíso, Valparaíso, Chile

[2] Program of Molecular and Clinical Pharmacology, ICBM, Faculty of Medicine, University of Chile, Clasificador 7, Independencia, 1027 Santiago, Chile

[3] Center for Bioinformatics and Integrative Biology, Universidad Andrés Bello, Santiago, Chile

[4] Fundación Fraunhofer Chile, Las Condes, Chile

[5] NBCM, CNRS, Gif-sur-Yvette, France

Introduction

Down syndrome (DS) in humans results from the trisomy of autosome 21. The condition constitutes the major genetic cause of mental retardation to survive birth. This condition determines an increased incidence of congenital malformations, muscle hypotonia, and an early onset of Alzheimer's disease neuropathology (Epstein 1986). Such abnormalities are a consequence of gene overdose determined by the extra copy of chromosome 21. Human chromosome 21 was the second human autosome to be fully sequenced (Hattori et al. 2000), an analysis which identified 127 genes and 98 new genes, which may potentially be overexpressed in DS. The syndrome requires as a minimum the presence of a portion located at the end of the long arm of chromosome 21 (namely, from bands 21q22.1 to qter), referred to as the DS critical region. However, in spite of the accumulated knowledge to date, the consequences of the overexpression of

specific DS-related gene products to altered cell function remains poorly understood (Saud et al. 2006). Hence, understanding the effect of overexpressed genes in chromosome 21, specifically those located in the aforementioned critical region, is of utmost importance to understand DS pathophysiology.

Among the genes located in the DS critical region is Slc5a3, encoding for the Na^+/myo-inositol cotransporter-1 (SMIT1) (Berry et al. 1995). The overexpression of SMIT1 has been related to high intracellular levels of myo-inositol in the brains of DS patients (Shonk and Ross 1995; Berry et al. 1999; Huang et al. 1999; Beacher et al. 2005). In mice, the Slc5a3 gene is localized in the telomeric region of chromosome 16 (McVeigh et al. 2000). Brains of trisomy 16 mice (Ts16), an animal model of DS, also exhibit increased myo-inositol levels (Shetty et al. 1996), and cultured neurons derived from this mouse model exhibit increased rates of myo-inositol uptake (Acevedo et al. 1997). Further, Ts65Dn mice, another model of DS, have been shown to also exhibit increased levels of myo-inositol in several regions of the central nervous system, as well as in non-neuronal tissue such as skeletal muscle and liver (Shetty et al. 2000) possibly due to increased uptake from extracellular compartments.

In spite of the current information on disrupted myo-inositol metabolism in DS and its animal models, little is known about its relation to specific cell dysfunction in the aneuploid condition. Myo-inositol is a known precursor for inositol lipid synthesis and an important osmolyte (Fisher et al. 2002). Therefore, abnormal levels of myo-inositol could potentially affect membrane metabolism, intracellular signaling, and cellular osmolarity, consequently disrupting neuronal functions.

As previously stated, Ts16 is a model of human DS. Regrettably, such animals are unviable, and they do not survive gestation. The development of mice with partial trisomy of autosome 16 (i.e., Ts65Dn and Ts1Cje) has overcome the issue of lethality, providing animals that survive gestation. More importantly, the new partial trisomic models have managed to eliminate excess dosage of genes present in murine autosome 16 that are unrelated to DS and in this fashion circumvent possible non-specific effects of the full murine trisomy. For these reasons, they are most powerful research models, in particular because they can be used in relevant behavioral studies. But, conversely, such models do not overexpress critical DS-related genes (i.e., Ts1Cje exhibits normal Sod1 levels) (Sago et al. 1998), and some lack the characteristic degeneration of basal forebrain cholinergic neurons (Sago et al. 1998). In order to overcome the lethality at least at the in vitro level and retain the most of the gene complement closest to the full trisomic condition in man, we have established a continuously growing cell line from cultured neurons from the cerebral cortex of trisomy 16 fetal mice. This cell line, named CTb, has been shown to exhibit increased resting cytosolic Ca^{2+} levels ($[Ca^{2+}]_c$) and slower time-dependent kinetics in the decay of $[Ca^{2+}]_c$ responses induced by neurotransmitter agonists, as compared with cells of the CNh cell line, established from the cerebral cortex of a normal euploid littermate. Such alterations are comparable to those seen in neurons cultured from Ts16 brains (Schuchmann et al., 1998), suggesting that in our trisomic cell line, this dysfunction is also present. $[Ca^{2+}]_c$ modulates different functions in the central nervous system, including neurotransmission, learning, and memory (Cárdenas et al. 1999). Since myo-inositol is a key precursor of phosphoinositide signaling, which acts via modulation of neuronal Ca^{2+} levels, we decided to study the contribution of SMIT1 overexpression to the impaired $[Ca^{2+}]_c$ dynamics in CTb cells. To achieve this goal, we reduced SMIT1 expression by transfecting CTb cells with specific messenger RNA (mRNA) antisense sequences, to levels comparable to those of the normal CNh line ("knockdown") (Opazo et al. 2006; Rojas et al. 2008). $[Ca^{2+}]_c$ measurements showed that SMIT1 knockdown corrects certain parameters of Ca^{2+} responses induced by glutamatergic and cholinergic agonists.

Materials and Methods

Culture of Cell Lines

The establishment, culture conditions, and characterization of the CNh and CTb cell lines are reported elsewhere (Allen et al. 2000; Cárdenas et al. 1999; Opazo et al. 2006; Rojas et al. 2008). Briefly, for standard growth conditions, cells were kept in feeding medium, composed of DMEM/Ham F12 nutrient mixture (1:1) modified to contain 6 g/l glucose, supplemented with 10% adult bovine serum and 2.5% fetal bovine serum (Opazo et al. 2006; Rojas et al. 2008). For recording of Ca^{2+} signals, cells were detached with 0.1% trypsin (Gibco, Grand Island, NY) and seeded onto round 25-mm-diameter glass coverslips or 35-mm-diameter plastic culture dishes, and media were renewed completely twice a week (Rojas et al. 2008).

For differentiation, prior to transfection and recording, the cultures were kept for 1 week in differentiating media as previously reported (Rojas et al. 2008). The media were composed of DMEM/ Ham F12 nutrient mixture (1:1) modified to contain 6 g/l glucose, supplemented with 1% fetal bovine serum.

SMIT1 Knockdown

SMIT1 knockdown was achieved using a specific phosphorothioate mRNA antisense sequence, which was designed considering a previously described antisense sequence complementary to a region of the rat SMIT1 mRNA (Lubrich et al. 2000), with modifications to complement with the

corresponding sequence in the mouse mRNA. The anti-SMIT1 sequence utilized, called As-SMIT1, was: 5′-TACG GCAATGTCTGCTGCCT-3. For specificity control, we designed a scrambled sequence, Sc-SMIT1, composed of the same amino acids present in As-SMIT1, randomly rearranged. The resulting final sequence was 5′-GCTCTGCTGCTCAT AGCTAG-3′.

CTb and CNh were cultured until reaching 80% confluence. Antisense or scrambled sequences (50 μM) were transfected into CTb cells using cationic liposomes (Lipofectamine™; Invitrogen, Inc., Fredericksburg, MD, USA) according to recommendations by the manufacturer with modifications previously described (Opazo et al. 2006; Rojas et al. 2008) In non-transfected cells, cultures were maintained in 500 μL DME/F12 media. Afterwards, the cultures were incubated at 37 °C, 5% CO_2, and 100% humidity for 5 h. Transfections were arrested by addition of 1 ml DMEM/F12 supplemented with adult bovine serum (10%, *v*/*v*), fetal bovine serum (2.5%, *v*/*v*), and gentamicin 40 mg/l (Opazo et al. 2006).

Determination of SMIT1 Protein Levels

SMIT1 protein contents were determined after 24, 48, and 72 h post-transfection with the aforementioned respective antisense sequences, using immunoblot, as previously reported (Opazo et al. 2006; Rojas et al. 2008). Briefly, the cells were washed in PBS composed of (mM) NaCl 130, KCl 5.4, Na_2HPO_4 0.14, and KH_2PO_4 0.22, pH 7.4, and detached by incubation with a trypsin-EDTA 0.1% solution for 3–5 min at 37 °C. The cells were then lysed in RIPA lyses buffer composed of (mM) NaCl 150, sodium deoxycolate 24, SDS 0.1% (*v*/*v*), Nonidet 1% (*v*/*v*), EDTA 250, and Tris Base 100, along with protease inhibitors (PMSF, leupeptine). Protein content was determined using the Bradford method. Eight micrograms of proteins were separated by SDS-PAGE on 12% polyacrylamide gels and transferred electrophoretically to nitrocellulose membranes. For blocking, the blots were incubated with 3% skim milk and Tween-20 1% for 1 h at room temperature. Afterwards, the membranes were incubated at 4 °C overnight with a primary anti-SMIT1 antibody (1:1000 chicken anti-SLC5A3; Genetel Laboratories LLC, Madison, WI). Afterwards, the membranes were washed and incubated with secondary antibodies (1:2000 anti-chicken IgY, Genetel Laboratories LLC, Madison, WI). Final detection was carried out using a chemiluminescence kit (GE Healthcare Bio-Sciences Corp., Piscataway, NJ, USA). As a loading control, we used β-tubulin expression, assessed by stripping the blots with 100 mM β-mercaptoethanol, 2% (*w*/*v*) SDS, and 62.5 mM Tris-HCl (pH 6.8 at 20 °C) and subsequently incubating with monoclonal β-tubulin antibody (anti-mouse β-tubulin, Sigma, Saint Louis, MI) overnight at 4 °C, followed by detection as detailed above. Finally, the membranes were scanned at 900 dpi and saved in a personal computer for later analysis. Pixel density analysis of the resulting bands was carried out by the image analysis software ImageJ (Natl. Institutes of Health, Bethesda, MD), by means of a customized gel analysis macro.

Cytosolic Ca^{2+} Studies

Variations in $[Ca^{2+}]_c$ were determined in cells loaded with Indo-1, as previously described (Montiel et al. 2003). Briefly, the cells plated in coverslips were incubated with 10 μg/ml Indo-1 acetoxymethyl ester (Molecular Probes, Invitrogen, Carlsbad, CA) at 37° for 40 min. Afterwards, the coverslips were washed with Krebs-HEPES buffer solution composed of (in mM) 140 NaCl, 5 KCl, 2 $MgCl_2$, 1.5 or 2.5 $CaCl_2$, HEPES-NaOH, and 10 dextrose (pH = 7.4). The coverslips were then mounted in a perfusion chamber placed on the stage of a fluorescence inverted microscope (Diaphot 200, Nikon Corp., Tokyo, Japan) equipped with two dichroic mirrors. One dichroic mirror sent the excitation light (355 nm) to the cells and the fluorescent light emitted by Indo-1 inside the cells (>400 nm) to the second mirror. In turn, this second dichroic mirror split the fluorescent light into beams centered at 410 and 485 nm, respectively. The light from each fluorescent signal was continuously monitored by two separate photomultipliers. Data were acquired and analyzed using a customized pCLAMP 8.1 software (Molecular Devices, Union City, CA).

Neurotransmitter agonists were applied externally using a custom-made pressure-driven microinjection system. The stimulus pipette, which had a tip diameter of ca. 1 μm, was filled with agonist solutions (glutamate or nicotine) and positioned at 10–15 μm from the cell for microinjection.

$[Ca^{2+}]_c$ signal amplitudes were measured from the baseline prior to stimuli, up to the peak of the response, as previously described (Cárdenas et al. 1999; Rojas et al. 2008). For decay analysis of the Ca^{2+} responses (after the peak), experimental curves were fitted to a one exponential function using the least square fit method. Statistical analysis was performed using one-way ANOVA, followed by an unpaired Student's *t* test (two-tailed) for individual comparisons.

Results

Effect of As-SMIT1 in the Expression of SMIT1

At first, we evaluated the expression of SMIT1 on CTb cells. As shown in Fig. 1, SMIT1 levels were elevated in CTb cells by 1.45-fold compared to CNh cells, after correcting with the load control β-tubulin (Fig. 1a). SMIT1/β-tubulin expression ratios were 0.75 ± 0.06 and 1.09 ± 0.07 for CNh and CTb cells, respectively ($p < 0.05$). This result correlates adequately with the expected gene dosage (Shetty et al. 1996). No

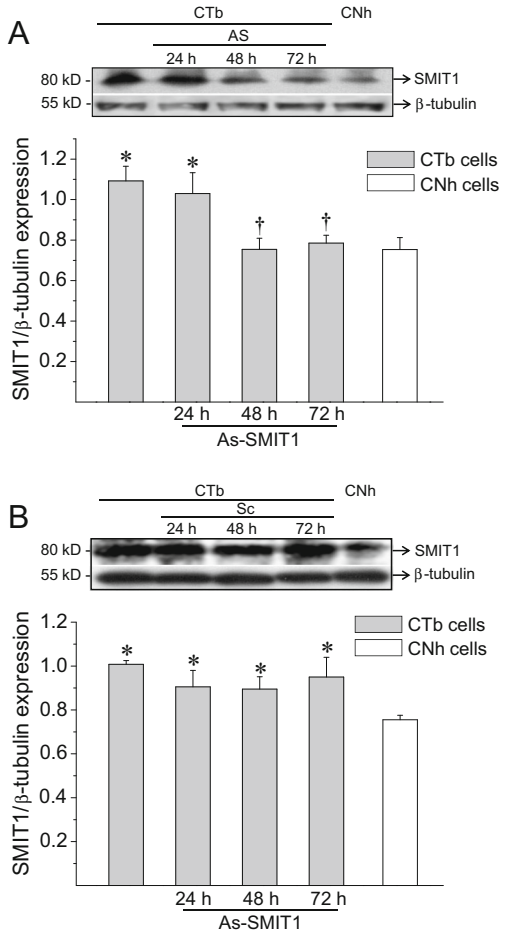

Fig. 1 SMIT1 overexpression is reduced in CTb cells as a result of transfection with a specific antisense. Antisenses were transfected into CTb cells using cationic liposomes, as detailed in the "Materials and Methods" section. SMIT1 expression was determined by immunoblot after 24, 48, and 72 h of transfection. β-Tubulin was utilized as a loading control. **a**, **b** present normalized SMIT1 expression in CNh cells (*white*) and CTb (*gray*) cells non-transfected or transfected with As-SMIT1 (**a**) or Sc-SMIT1 (**b**). *Bars* represent means ± SEM; $n = 4$. *$p < 0.05$ compared to non-treated CTb cells; †$p < 0.05$ compared with non-transfected CTb cells (one way-ANOVA followed by *t* test). *Inset*: representative immunoblots

significant effects were observed 24 h after transfection with As-SMIT1. However, 48 and 72 h post-transfection, the As-SMIT1 sequence significantly reduced SMIT1 expression in CTb cells, taking it to levels comparable to those of CNh cells. SMIT1/β-tubulin expression ratios were 0.75 ± 0.06 and 0.79 ± 0.04 at 48 and 72 h post-transfection, respectively. Both values were significantly lower as compared with non-transfected CTb cells ($p < 0.05$). On the other hand, transfection of CTb cells with the control Sc-SMIT1 sequence had no effect in reducing SMIT1 expression in all time periods studied (Fig. 1b), thus verifying the specific effect of As-SMIT1.

Since SMIT1 levels in As-SMIT1-transfected CTb cells remained similar to those of CNh up to 48 h post-transfection, we chose this time to assess the effect of the SMIT1 knockdown on $[Ca^{2+}]_c$.

SMIT1 Knockdown Did Not Affect Resting Cytosolic Ca^{2+} Levels in CTb Cells

As we had previously reported (Cárdenas et al. 1999), CTb cells exhibited higher resting $[Ca^{2+}]_c$, compared to those of CNh cells. Resting $[Ca^{2+}]_c$ values for CNh and CTb cells were 138 ± 5 and 176 ± 6 nM, respectively, being significantly different ($p < 0.05$). As shown in Fig. 2, transfection of CTb cells with either As-SMIT1 or Sc-SMIT1 did not modify the resting $[Ca^{2+}]_c$. Resting $[Ca^{2+}]_c$ values for CTb cells transfected with As-SMIT1 or Sc-SMIT1 were 178 ± 5 and 185 ± 4 nM, respectively. Both values were significantly greater than those determined for resting $[Ca^{2+}]_c$ of CNh cells ($p < 0.05$).

SMIT1 Knockdown Decreases the Amplitude and Accelerates Decay Kinetics of Glutamate-Induced $[Ca^{2+}]_c$ Signals in CTb Cells

Since glutamate is one of the most important excitatory neurotransmitters in the nervous system and it is essential for higher functions such as learning and memory, we studied the effect of SMIT1 knockdown on the $[Ca^{2+}]_c$ rise induced by glutamate. Figure 3a shows representative $[Ca^{2+}]_c$ signals in response to glutamate in CTb and CNh cells. In agreement with previous results obtained by our group (Cárdenas et al. 1999), $[Ca^{2+}]_c$ signals in CTb cells evidenced larger amplitudes and slower decay kinetics, in relation to signals observed in euploid CNh cells. Indeed, amplitudes of $[Ca^{2+}]_c$ signals induced by glutamate in CNh and CTb cells were 1.7 ± 0.2 and 3.6 ± 0.4 μM, respectively, being significantly greater in CTb cells ($p < 0.05$). Decay time constants of the $[Ca^{2+}]_c$ signals were 4.3 ± 0.4 and 5.9 ± 0.3 s^{-1} for CNh and CTb cells, respectively, being significantly slower for CTb cells ($p < 0.05$).

Figure 3b shows that SMIT1 knockdown dramatically reduced the $[Ca^{2+}]_c$ rise induced by glutamate, to levels comparable to those observed in CNh cells. The amplitude of the $[Ca^{2+}]_c$ signal induced by glutamate in CTb cells transfected with As-SMIT1 was 1.4 ± 0.2 μM. These values were significantly reduced compared to $[Ca^{2+}]_c$ signal amplitude values in non-transfected CTb cells ($p < 0.05$). The amplitude of the glutamate-induced $[Ca^{2+}]_c$ signal in CTb cells with SMIT1 knockdown was also significantly lower than those of CTb cells transfected with As-SMIT1 ($p < 0.05$), whose value was 2.4 ± 0.2 μM.

Regarding time-dependent kinetics of the decay phase, Fig. 3c shows that As-SMIT1 transfection of CTb cells also accelerated the decay phase of the glutamate-induced $[Ca^{2+}]_c$ signals. Indeed, the decay time constant of the $[Ca^{2+}]_c$ signals in this latter condition was 4.5 ± 0.3 s^{-1}, a value significantly slower as compared with that of non-transfected CTb cells ($p < 0.05$), as well as compared with the decay time constant of cells transfected with Sc-SMIT1 ($p < 0.05$). The decay time

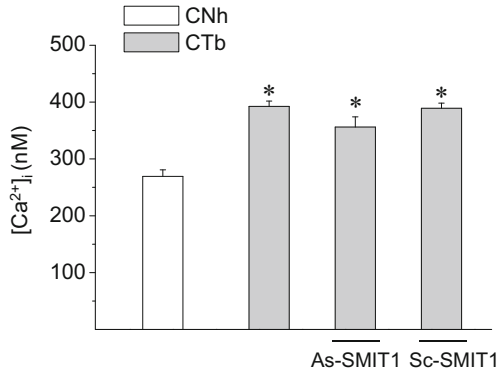

Fig. 2 SMIT1 knockdown did not affect resting $[Ca^{2+}]_c$ in CTb cells. CTb cells were transfected with As-SMIT1 or Sc-SMIT1 as detailed in the "Materials and Methods" section. Resting $[Ca^{2+}]_c$ was determined in Indo-1-loaded cells 48 h post-transfection. The bar graphs show means ± SE (40–45 cells) of resting $[Ca^{2+}]_c$ in CNh cells (*white*) or CTb cells (*gray*) non-transfected or transfected with As-SMIT1 or Sc-SMIT1. *$p < 0.05$ compared with CNh cells (one way-ANOVA followed by *t* test)

constant of the $[Ca^{2+}]_c$ signals of CTb cells transfected with Sc-SMIT1 was 5.7 ± 0.4 s^{-1}.

SMIT1 Knockdown Accelerates the Decay Kinetics of Cholinergic Agonists-Induced $[Ca^{2+}]_c$ Signals in CTb Cells

Since CTb and CNh cells exhibit cholinergic-induced $[Ca^{2+}]_c$ signals (Cárdenas et al. 1999; Rojas et al. 2008), we then evaluated the effects of SMIT1 knockdown on $[Ca^{2+}]_c$ signals induced by cholinergic receptor agonists, namely muscarine and nicotine (Cárdenas et al. 1999). Our aim was to compare the effects of SMIT1 knockdown on the $[Ca^{2+}]_c$ induced by the activation of these receptors.

Figure 4a shows representative $[Ca^{2+}]_c$ signals induced by nicotine in CTb and CNh cells. Nicotine induced an increase in the $[Ca^{2+}]_c$ signals with amplitudes of 1.5 ± 0.1 μM for CNh and 1.3 ± 0.1 μM for CTb, although the differences among CNh and CTb cells were not statistically significant (Fig. 4b). Transfection of CTb cells with As-SMIT1 or Sc-SMIT1 did not affect nicotinic-induced $[Ca^{2+}]_c$ signal amplitudes; which exhibited values of 1.5 ± 0.1 and 1.4 ± 0.1 μM, respectively.

On the other hand, a slower decay phase of the nicotinic-induced $[Ca^{2+}]_c$ signal was evident in CTb cells (Fig. 4c). Decay time constants of the $[Ca^{2+}]_c$ signals were 2.3 ± 0.1 and 6.8 ± 0.2 s^{-1} for CNh and CTb cells, respectively, being significantly slower for CTb cells ($p < 0.05$). The slower decay kinetics in CTb cell $[Ca^{2+}]_c$ signals was reverted to levels comparable to those of CNh cells, after 48 h of transfection with As-SMIT1 (Fig. 4c). The decay time constant in this latter condition was 2.8 ± 0.1 s^{-1}, a value significantly slower as compared with the decay kinetics of CTb cells non-transfected and transfected with Sc-SMIT1 ($p < 0.05$). The

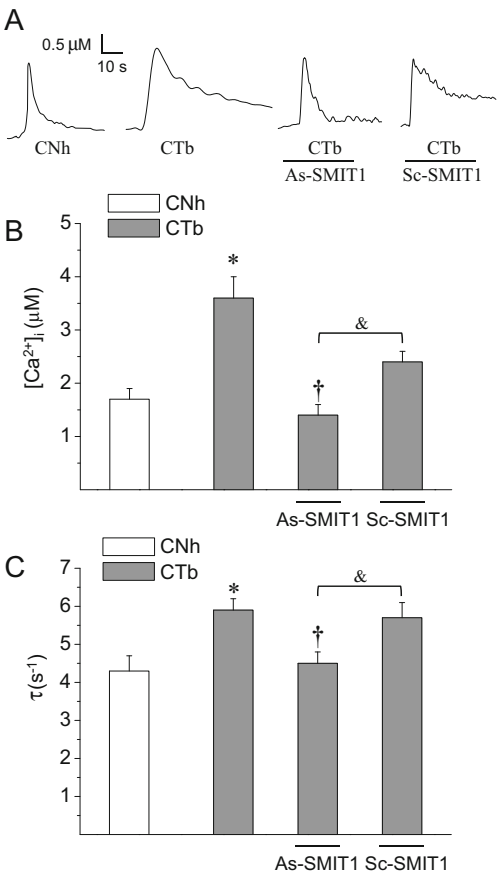

Fig. 3 SMIT1 knockdown normalizes amplitude and decay kinetics of glutamate-induced $[Ca^{2+}]_c$ signals in CTb cells. CTb cells were transfected with As-SMIT1 or Sc-SMIT1 as detailed in "Materials and Methods" section. Forty-eight hours after transfection, cells were loaded with Indo-1 and stimulated with glutamate (300 μM). **a** Representative recording of glutamate-induced $[Ca^{2+}]_c$ signals in both CNh or CTb cells non-transfected or transfected with As-SMIT1 or Sc-SMIT1. Bar graphs show means ± SE (12–14 cells) of amplitude (**b**) and decay time constant τ (**c**) of glutamate-induced $[Ca^{2+}]_c$ signals in CNh cells (*white*) or CTb cells (*gray*) non-transfected or transfected with As-SMIT1 or Sc-SMIT1. *$p < 0.05$ compared with CNh cells; †$p < 0.05$ compared with non-transfected CTb cells, &$p < 0.05$ compared with As-SMIT1-transfected cells (one way-ANOVA followed by *t* test)

decay time constant of the $[Ca^{2+}]_c$ signals of CTb cells transfected with Sc-SMIT1 was 7.2 ± 0.1 s^{-1}.

Figure 5a shows representative $[Ca^{2+}]_c$ signals induced by muscarine in CTb and CNh cells. Amplitudes of the muscarine-induced $[Ca^{2+}]_c$ signals were 0.5 ± 0.04 and 1.4 ± 0.2 μM for CNh and CTb cells, respectively, being significantly higher in the trisomic CTb cells ($p < 0.05$). However, SMIT1 knockdown had no effect on the amplitude of $[Ca^{2+}]_c$ signals in CTb cells (Fig. 5b). Amplitudes of the muscarine-induced $[Ca^{2+}]_c$ signals were 1.6 ± 0.2 and 1.4 ± 0.2 μM for CTb cells transfected with As-SMIT1 or Sc-SMIT1, respectively.

In a manner similar to that of nicotine stimulation, decay kinetics of the $[Ca^{2+}]_c$ signals induced by muscarine were significantly slower in the trisomic CTb cells, as compared

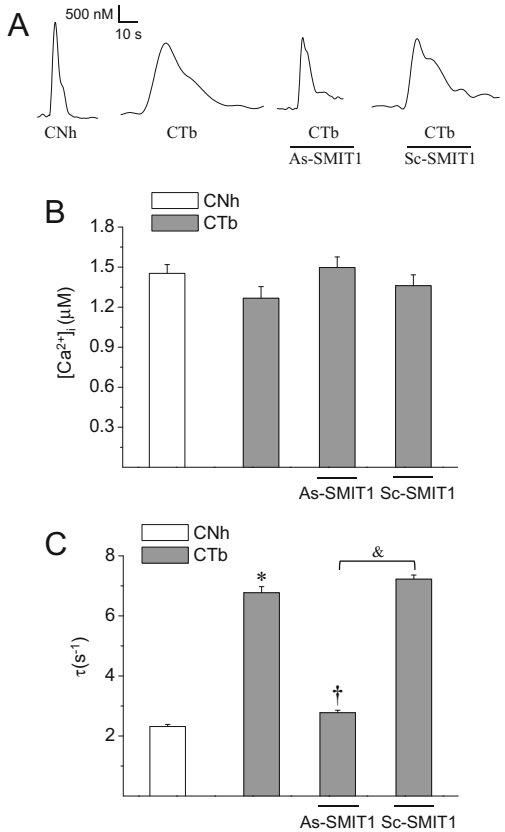

Fig. 4 SMIT1 knockdown normalizes decay kinetics of $[Ca^{2+}]_c$ signals induced by nicotine in CTb cells. CTb cells were transfected with As-SMIT1 or Sc-SMIT1 as detailed in the "Materials and Methods" section. Forty-eight hours after transfection, cells were loaded with Indo-1 and stimulated with nicotine (300 μM). **a** Representative recordings of nicotine-induced $[Ca^{2+}]_c$ signals in CNh cells or CTb cells non-transfected or transfected with As-SMIT1 or Sc-SMIT1. Bar graphs show means ± SE (10–12 cells) of the amplitude (**b**) and decay time constant τ (**c**) of nicotine-induced $[Ca^{2+}]_c$ responses in CNh (*white*) or CTb cells (*gray*) non-transfected or transfected with As-SMIT1 or Sc-SMIT1. *$p < 0.05$ compared with CNh cells; †$p < 0.05$ compared with non-transfected CTb cells, &$p < 0.05$ compared with As-SMIT1-transfected cells (one way-ANOVA followed by *t* test)

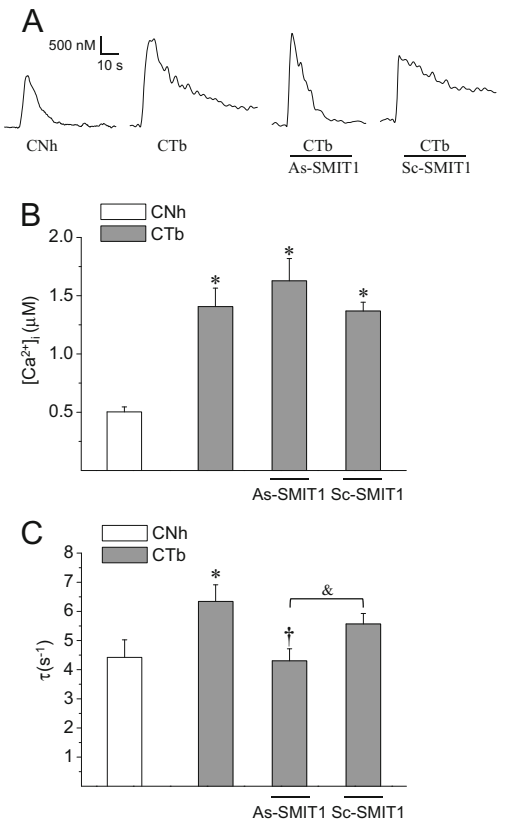

Fig. 5 SMIT1 knockdown normalizes decay kinetics of $[Ca^{2+}]_c$ signals induced by muscarine in CTb cells. CTb cells were transfected with As-SMIT1 or Sc-SMIT1 as detailed in the "Materials and Methods" section. Forty-eight hours after transfection, cells were loaded with Indo-1 and stimulated with nicotine (300 μM). **a** Representative recordings of nicotine-induced $[Ca^{2+}]_c$ signals in CNh or CTb cells non-transfected or transfected with As-SMIT1 or Sc-SMIT1. Bar graphs show means ± SE (12–14 cells) of the amplitude (**b**) and decay time constant τ (**c**) of nicotine-induced $[Ca^{2+}]_c$ responses in CNh cells (*white*) or CTb cells (*gray*) non-transfected or transfected with As-SMIT1 or Sc-SMIT1. *$p < 0.05$ compared with CNh cells, †$p < 0.05$ compared with non-transfected CTb cells, &$p < 0.05$ compared with As-SMIT1-transfected cells (one way-ANOVA followed by *t* test)

with their control CNh cells; these values were 4.4 ± 0.6 and 6.3 ± 0.3 s^{-1} for CNh and CTb cells, respectively ($p < 0.05$). With this stimulus, the SMIT1 knockdown significantly reduced the decay time constant to levels essentially comparable to those of CNh (Fig. 5c). Indeed, the decay time constant of CTb cells transfected with Sc-SMIT1 was 4.3 ± 0.4 s^{-1}, a value significantly smaller compared with the decay kinetics of CTb cells non-transfected and transfected with Sc-SMIT1 ($p < 0.05$). The decay time constant of the $[Ca^{2+}]_c$ signals of CTb cells transfected with Sc-SMIT1 was 5.6 ± 0.4 s^{-1}.

Discussion

SMIT1 gene (Slc5a3) is one of the genes located in the DS critical region, causing the overexpression of this protein with the consequently augmented brain concentration of myo-inositol (Shetty et al. 1996, 2000). Such increased brain myo-inositol levels have been associated with reduced cognitive ability in DS patients (Beacher et al. 2005). In the present work, we observed that SMIT1 is significantly overexpressed in the CTb cell line, compared to euploid CNh cells. Indeed, we estimated that SMIT1 expression in CTb cells is 45% higher, compared to CNh cells, a value that agrees with the increased gene dosage that characterizes the trisomic condition. Thus, our CTb cell line could constitute an adequate model to study the contribution of the overexpressed SMIT1 to the altered cellular functions associated with the trisomic condition (Saud et al. 2006).

Transfection of CTb cells with the specific SMIT1 antisense caused a significant reduction on SMIT1 protein abundance, which was comparable to the corresponding protein

level in CNh cells. Conversely, the use of the control Sc-SMIT1 sequence had no effect on SMIT1 expression. When SMIT1 protein expression in CTb cells attained levels essentially similar to those of the CNh control cell line, we studied the $[Ca^{2+}]_c$ responses that are reportedly impaired in primary cultures of neurons from trisomy 16 mice (Schuchmann et al., 1998) and also in our cell lines derived from murine cerebral cortex (Cárdenas et al. 1999; Rojas et al. 2008). Our current studies confirm that neurons from trisomic animals exhibit greater resting $[Ca^{2+}]_c$ levels and slower decay kinetics of agonist-induced $[Ca^{2+}]_c$ responses (Cárdenas et al. 1999; Schuchmann et al., 1998). We now show that SMIT1 knockdown in CTb cells significantly accelerated the decay kinetics of the $[Ca^{2+}]_c$ signals induced by glutamate, nicotine, and muscarine, to values similar to those of CNh cells. Further, knockdown of the transporter reduced the amplitude of glutamate-induced $[Ca^{2+}]_c$ signals, again to levels essentially comparable to those of CNh cells. However, no effect of SMIT1 knockdown on resting $[Ca^{2+}]_c$ was evident.

The overexpression of SMIT1 in Ts16 cells most likely results in high levels of myo-inositol, which has been observed in brains of Ts16 mice (Shetty et al. 1996). Further, recent evidence brought forth by in vivo proton magnetic resonance spectroscopy studies has confirmed the presence of increased myo-inositol content in the brain of Ts65Dn mice (Santin et al. 2014), previously reported by Huang et al. (2000). Similarly, and by the same technique, elevated myo-inositol has been reported in brains of DS patients (Berry et al. 1999; Lamar et al. 2011; Lin et al. 2016), compared to the respective normal controls. The latter studies show a correlation of increased levels of the metabolite and the degree of dementia in the affected individuals. One possible explanation for this correlation is that in the CNS, myo-inositol is considered a putative glial marker and that the imbalance of this metabolite may lead to an overall higher glial inflammatory component in the trisomic condition (Lin et al. 2016). Although our data generate from a neuronal model, similar alterations may arise from the imbalance and result in the Ca^{2+} responses reported herein. In the cell, elevated levels of myo-inositol could disrupt the phosphatidylinositol cycle, affecting the synthesis of Ins(1,4,5)P3 and Ca^{2+} release from intracellular stores, with the consequent alteration of cytosolic Ca^{2+} levels (Barbara 2002). Given that cytosolic Ca^{2+} influences diverse protein kinases, such as protein kinase A (PKA), protein kinase (PKC), and Ca^{2+}/calmodulin-dependent protein kinase, among others, the overexpression of SMIT1 would then impact on different Ca^{2+}-dependent kinase pathways and their substrates. For instance, the neuronal nicotinic receptor is phosphorylated in the α subunit by both PKA (Nakayama et al. 1993) and PKC (Downing and Role 1987). Depending on the nicotinic cholinergic receptor subtypes present in the SNC, the activation of the PKC favors the recovery from desensitized states (Fenster et al. 1999; Marszalec et al. 2005). In this way, a fraction of abnormally phosphorylated receptors could then recover faster, which in turn could be made available to bind acetylcholine and hence be activated again. In this fashion, the activation of the said receptors could determine changes in $[Ca^{2+}]_c$ signals that although not expressed in greater amplitude (Fig. 4b), could be sufficient to maintain a $[Ca^{2+}]_c$ rise for longer periods of time, as represented in a greater time constant of the decay phase kinetic in the trisomic condition (Fig. 4b). PKC also enhances channel activity and increases surface expression of both *N*-methyl-D-aspartate (NMDA) receptor (Lan et al. 2001; Popp et al. 2008) and alpha-amino-3-hydroxy-5-methyl-4-isoxazolepropionate (AMPA) receptors (Correia et al. 2003; Sun and June Liu 2007). Particularly, PKC activation increases the expression of functional NMDA receptor at the cell surface (Marszalec et al. 2005) and augments the amplitude of NMDA-induced currents (Popp et al. 2008). The activation of PKC also increases AMPA surface expression (Gomes et al. 2007). In this fashion, an increased activation of PKC, as a consequence of excess diacylglycerol in CTb cells, could increase NMDA and AMPA receptor levels at the cell membrane. The glutamate responses in our CTb and CNh cell lines mainly depend on NMDA and AMPA receptors (Cárdenas et al. 1999). Then, the activation of glutamate receptors in CTb cells could determine $[Ca^{2+}]_c$ responses with greater amplitudes, as observed by our group in a previous communication (Cárdenas et al. 1999) and in the present work (Fig. 3c). Interestingly, such altered $[Ca^{2+}]_c$ responses were normalized by the SMIT1 knockdown.

As aforementioned, increased levels of myo-inositol could also increase inositol 1,4,5-triphosphate (IP_3) production. As compared with the $[Ca^{2+}]_c$ increase originated by Ca^{2+} entry through channels or receptors, the $[Ca^{2+}]_c$ increase caused by activation of IP_3-sensitive receptors could be slow and sustained. In this regard, $[Ca^{2+}]_c$ responses in CTb cells, which depend on IP_3-sensitive receptor activation, should have slower decay kinetics. That is the case of $[Ca^{2+}]_c$ responses induced by muscarine (Fig. 5c), which activates metabotropic receptors with the consequent production of IP_3, and the subsequent release of Ca^{2+} from intracellular stores. As predicted then, SMIT1 knockdown normalized the decay kinetics of $[Ca^{2+}]_c$ responses induced by muscarine. Interestingly, excitatory ionotropic receptors, such as AMPA and nicotinic receptors, can also trigger the production of IP_3 with the consequent release of Ca^{2+} from intracellular stores (Okubo et al. 2001; Dickinson et al. 2007). This mechanism reportedly also contributes to the persistent elevation of $[Ca^{2+}]_c$ as a consequence of the activation of nicotinic receptors (Gueorguiev et al. 2000; Dajas-Bailador et al. 2002). In this fashion, overproduction of IP_3 in CTb cells can explain not only the slower decay kinetics of $[Ca^{2+}]_c$ responses induced by muscarine, but also those evoked by nicotine and glutamate (Figs. 3c and 4c). Interestingly, such decay kinetics

were normalized by the knockdown of SMIT1. However, we have previously demonstrated that stimulation with the aforementioned agonist results in Ca^{2+} signal increases that are dependent on extracellular Ca^{2+} (Cárdenas et al. 1999, Rojas et al. 2008), as removal of external Ca^{2+} results in the abolishment of the response. Hence, it is more likely that the effects of SMIT1 knockdown in this parameter are linked to other impairments in Ca^{2+} homeostasis, such as cell Ca^{2+} buffering and/or altered membrane receptor kinetics.

Recent evidence also links the overexpression of SMIT1 to regulation of the KCNQ2/3 K^+ channels, key players in membrane excitability (Dai et al. 2016). These authors demonstrated that total PI levels were unchanged in cells overexpressing the transporter. However, a reciprocal regulation has been reported in the brain between KCNQ1 and SMIT1, possibly related to the formation channel-transporter complexes (Abbott et al., 2014). Although such regulation is yet to be confirmed for KCNQ2/3, it is tempting to speculate that excess SMIT1 could be affecting K^+ channel activity and in turn neuronal excitability and hence partly explain our findings reported herein.

Our current results pose SMIT1 and the mechanisms that it influences as an interesting target from the pharmacological point of view. SMIT1 could result in increased intracellular myo-inositol concentration. In this regard, treatment with lithium has been shown to reduce myo-inositol levels in the brain of Ts65Dn animals (Huang et al. 2000) and, by the same token, rescue synaptic plasticity in the same animal model (Contestabile et al. 2013). Testing the effects of lithium in our cell models, and exploring its effects on the impairments in Ca^{2+} homeostasis described herein, may provide further mechanistic evidence of DS-related alterations, a possibility well worth exploring.

Finally, it is important to consider that several genes are overexpressed in the trisomic condition, and a number of them cooperatively contribute to the cellular alterations observed in this condition. In this regard, in a previous communication, we reported that the knockdown of the amyloid precursor protein, which is also overexpressed in the human and murine trisomic condition, restores normal $[Ca^{2+}]_c$ homeostasis in CTb cells (Rojas et al. 2008). Indeed, amyloid precursor protein knockdown reduced resting $[Ca^{2+}]_c$ and accelerated decay kinetics of $[Ca^{2+}]_c$ responses induced by either depolarization with high extracellular K^+, application of glutamatergic agonists, nicotine, or ionomycin. It seems, therefore, that excess amyloid precursor protein contributes to a general mechanism implicated in the deregulation of $[Ca^{2+}]_c$ homeostasis, whereas in light of our present results, the effect of SMIT1 knockdown on $[Ca^{2+}]_c$ signals seems to be more specific. However, independent of the underlying mechanisms, the overexpression of both SMIT1 and APP converges in common alterations related with $[Ca^{2+}]_c$ responses and homeostasis. Therefore, a potential therapy for DS should consider more than one target gene.

Conclusions

SMIT1 overexpression contributes to the altered Ca^{2+} signals observed in response to cholinergic and glutamatergic receptor activation in the cell line CTb, a cellular model of the DS. Then, the normalization of SMIT1 overexpression could constitute a relevant therapeutic target for treatment of the DS-related neuronal dysfunction, as well as the signaling pathways that are disturbed by the overexpressed transporter. Also, the cell membrane localization of the transporter and the neurotransmitter receptors studied herein provides even better access to potential modulating drugs.

Acknowledgments This study is funded by Fondecyt (Chile) grant nos. 1040862 and 1130241, Enlaces ENL 07/05 (Univ. of Chile), CNRS/Conicyt Exchange Program, Fondation J. Lejeune (France), and P09-022-F from ICM-ECONOMIA, Chile. The Centro Interdisciplinario de Neurociencia de Valparaíso (CINV) is a Millennium Institute supported by the Millennium Scientific Initiative of the Ministerio de Economía, Fomento y Turismo. Pablo Caviedes holds patent protection on the CNh and CTb cell lines. The authors wish to thank Mr. Fernando Guzmán for his valuable technical assistance.

References

Abbott GW, Tai KK, Neverisky DL, Hansler A, Hu Z, Roepke TK, Lerner DJ, Chen Q, Liu L, Zupan B, Toth M, Haynes R, Huang X, Demirbas D, Buccafusca R, Gross SS, Kanda VA, Berry GT (2014) KCNQ1, KCNE2, and Na+-coupled solute transporters form reciprocally regulating complexes that affect neuronal excitability (2014). Sci Signal 7:1–23

Acevedo LD, Holloway HW, Rapoport SI, Shetty HU (1997) Application of stable isotope tracer combined with mass spectrometric detection for studying myo-inositol uptake by cultured neurons from fetal mouse: effect of trisomy 16. J Mass Spectrom 32:395–400

Allen DD, Martin J, Arriagada C, Cárdenas AM, Rapoport SI, Caviedes R, Caviedes P (2000) Impaired cholinergic function in cell lines derived from the cerebral cortex of normal and trisomy 16 mice. Eur J Neurosci 12:3259–3264

Barbara JG (2002) IP3-dependent calcium-induced calcium release mediates bidirectional calcium waves in neurons: functional implications for synaptic plasticity. Biochim Biophys Acta 1600:12–18

Beacher F, Simmons A, Daly E, Prasher V, Adams C, Margallo-Lana ML, Morris R, Lovestone S, Murphy K, Murphy DG (2005) Hippocampal myo-inositol and cognitive ability in adults with Down syndrome: an in vivo proton magnetic resonance spectroscopy study. Arch Gen Psychiatry 62:1360–1365

Berry GT, Mallee JJ, Kwon HM, Rim JS, Mulla WR, Muenke M, Spinner NB (1995) The human osmoregulatory Na+/myo-inositol cotransporter gene (SLC5A3): molecular cloning and localization to chromosome 21. Genomics 25:507–513

Berry GT, Wang ZJ, Dreba SF, Finucane BM, Zimmerman RA (1999) In vivo brain myoinositol levels in children with Down syndrome. J Pediatr 135:94–97

Cárdenas AM, Rodríguez MP, Cortés MP, Alvarez RM, Wei W, Rapoport SI, Shimahara T, Caviedes R, Caviedes P (1999) Calcium signals in cell lines derived from the cerebral cortex of normal and trisomy 16 mice. Neuroreport 10:363–369

Contestabile A, Greco B, Ghezzi D, Tucci V, Benfenati F, Gasparini L (2013) Lithium rescues synaptic plasticity and memory in Down syndrome mice. J Clin Invest 123(1):348–361

Correia SS, Duarte CB, Faro CJ, Pires EV, Carvalho AL (2003) Protein kinase C gamma associates directly with the GluR4 alpha-amino-3-hydroxy-5-methyl-4-isoxazole propionate receptor subunit. Effect on receptor phosphorylation. J Biol Chem 278:6307–6313

Dai G, Yu H, Kruse M, Traynor-Kaplan A, Hille B (2016) Osmoregulatory inositol transporter SMIT1 modulates electrical activity by adjusting PI(4,5)P2 levels. Proc Natl Acad Sci U S A 113: E3290–E3299

Dajas-Bailador FA, Mogg AJ, Wonnacott S (2002) Intracellular Ca2+ signals evoked by stimulation of nicotinic acetylcholine receptors in SH-SY5Y cells: contribution of voltage-operated Ca2+ channels and Ca2+ stores. J Neurochem 81:606–614

Dickinson JA, Hanrott KE, Mok MH, Kew JN, Wonnacott S (2007) Differential coupling of alpha7 and non-alpha7 nicotinic acetylcholine receptors to calcium-induced calcium release and voltage-operated calcium channels in PC12 cells. J Neurochem 100:1089–1096

Downing JE, Role LW (1987) Activators of protein kinase C enhance acethylcholine receptor in sympathetic ganglion neurons. Proc Natl Acad Sci U S A 84:7739–7773

Epstein CJ (1986) In: Epstein CJ (ed) Introduction in the neurobiology of Down syndrome. Raven Press, N. Y, pp 1–15

Fenster CP, Beckman ML, Parker JC, Sheffield EB, Whitworth TL, Quick MW, Lester RA (1999) Regulation of alpha4beta2 nicotinic receptor desensitization by calcium and protein kinase C. Mol Pharmacol 55:432–443

Fisher SK, Novak JE, Agranoff BW (2002) Inositol and higher inositol phosphates in neural tissues: homeostasis, metabolism and functional significance. J Neurochem 82:736–754

Gomes AR, Correia SS, Esteban JA, Duarte CB, Carvalho AL (2007) PKC anchoring to GluR4 AMPA receptor subunit modulates PKC-driven receptor phosphorylation and surface expression. Traffic 8: 259–269

Gueorguiev VD, Zeman RJ, Meyer EM, Sabban EL (2000) Involvement of alpha7 nicotinic acetylcholine receptors in activation of tyrosine hydroxylase and dopamine beta-hydroxylase gene expression in PC12 cells. J Neurochem 75:1997–2005

Hattori M, Fujiyama A, Taylor TD, Watanabe H, Yada T, Park HS, Toyoda A, Ishii K, Totoki Y, Choi DK, Groner Y, Soeda E, Ohki M, Takagi T, Sakaki Y, Taudien S, Blechschmidt K, Polley A, Menzel U, Delabar J, Kumpf K, Lehmann R, Patterson D, Reichwald K, Rump A, Schillhabel M, Schudy A, Zimmermann W, Rosenthal A, Kudoh J, Schibuya K, Kawasaki K, Asakawa S, Shintani A, Sasaki T, Nagamine K, Mitsuyama S, Antonarakis SE, Minoshima S, Shimizu N, Nordsiek G, Hornischer K, Brant P, Scharfe M, Schon O, Desario A, Reichelt J, Kauer G, Blocker H, Ramser J, Beck A, Klages S, Hennig S, Riesselmann L, Dagand E, Haaf T, Wehrmeyer S, Borzym K, Gardiner K, Nizetic D, Francis F, Lehrach H, Reinhardt R, Yaspo ML (2000) The DNA sequence of human chromosome 21. Nature 405:311–319

Huang H, Alexander GE, Daly EM, Shetty HU, Krasuski JS, Rapoport SI, Schapiro MB (1999) High brain myo-inositol levels in the predementia phase of Alzheimer's disease in adults with Down's syndrome: a 1H-MRS study. Am J Psychiatry 156:1879–1886

Huang W, Galdzicki Z, van Gelderen P, Balbo A, Chikhale EG, Schapiro MB, Rapoport SI (2000) Brain myo-inositol level is elevated in Ts65Dn mouse and reduced after lithium treatment. Neuroreport 11:445–448

Lamar M, Foy CM, Beacher F, Daly E, Poppe M, Archer N, Prasher V, Murphy KC, Morris RG, Simmons A, Lovestone S, Murphy DG (2011) Down syndrome with and without dementia: an in vivo proton magnetic resonance spectroscopy study with implications for Alzheimer's disease. NeuroImage 57:63–68

Lan JY, Skeberdis VA, Jover T, Grooms SY, Lin Y, Araneda RC, Zheng X, Bennett MV, Zukin RS (2001) Protein kinase C modulates NMDA receptor trafficking and gating. Nat Neurosci 4:382–390

Lin AL, Powell D, Caban-Holt A, Jicha G, Robertson W, Gold BT, Davis R, Abner E, Wilcock DM, Schmitt FA, Head E (2016) (1)H-MRS metabolites in adults with Down syndrome: effects of dementia. Neuroimage Clin 2:728–735

Lubrich B, van Calker D, Peschka-Süss R (2000) Inhibition of inositol uptake in astrocytes by antisense oligonucleotides delivered by pH-sensitive liposomes. Eur J Biochem 267:2432–2438

Marszalec W, Yeh YZ, Narahashi T (2005) Desensitization of nicotine acetylcholine receptors: modulation by kinase activation and phosphatase inhibition. Eur J Pharmacol 514:83–90

McVeigh KE, Mallee JJ, Lucente A, Barnoski BL, Wu S, Berry GT (2000) Murine chromosome 16 telomeric region, homologous with human chromosome 21q22, contains the osmoregulatory Na(+)/myo-inositol cotransporter (SLC5A3) gene. Cytogenet Cell Genet 88:153–158

Montiel C, Mendoza I, Garcia CJ, Awad Y, García-Olivares J, Solís-Garrido LM, Lara H, García AG, Cárdenas AM (2003) Distinct protein kinases regulate SNAP-25 expression in chromaffin cells. J Neurosci Res 71:353–364

Nakayama H, Okuda H, Nakashima T (1993) Phosphorylation of rat brain nicotinic acetylcholine receptor by cAMP-dependent protein kinase in vitro. Brain Res Mol Brain Res 20:171–177

Okubo Y, Kakizawa S, Hirose K, Iino M (2001) Visualization of IP(3) dynamics reveals a novel AMPA receptor-triggered IP(3) production pathway mediated by voltage-dependent Ca2+ influx in Purkinje cells. Neuron 32:113–122

Opazo P, Saud K, de Saint Pierre M, Cárdenas AM, Allen DD, Segura-Aguilar J, Caviedes R, Caviedes P (2006) Knockdown of amyloid precursor protein normalizes cholinergic function in a cell line derived from the cerebral cortex of a trisomy 16 mouse, an animal model of Down syndrome. J Neurosci Res 84:13031310

Popp RL, Reneau JC, Brotherton BJ (2008) Activation of protein kinase C enhances NMDA-induced currents in primary cultured cerebellar granule cells: effect of temperature and NMDA NR2 subunit composition. Eur J Pharmacol 599:1–10

Rojas G, Cárdenas AM, Fernández-Olivares P, Shimahara T, Segura-Aguilar J, Caviedes R, Caviedes P (2008) Effect of the knockdown of amyloid precursor protein on intracellular calcium increases in a neuronal cell line derived from the cerebral cortex of a trisomy 16 mouse. Exp Neurol 209:234–242

Sago H, Carlson EJ, Smith DJ, Kilbridge J, Rubin EM, Mobley WC, Epstein CJ, Huang TT (1998) Ts1Cje, a partial trisomy 16 mouse model for Down syndrome, exhibits learning and behavioral abnormalities. Proc Natl Acad Sci USA 95:6256–6261

Santin MD, Valabrègue R, Rivals I, Pénager R, Paquin R, Dauphinot L, Albac C, Delatour B, Potier MC (2014) In vivo 1H MRS study in microlitre voxels in the hippocampus of a mouse model of Down syndrome at 11.7 T. NMR Biomed 27:1143–1150

Saud K, Arriagada C, Cárdenas AM, Shimahara T, Allen DD, Caviedes R, Caviedes P (2006) Neuronal dysfunction in Down syndrome: contribution of neuronal models in cell culture. J Physiol Paris 99: 201–210

Schuchmann S, Müller W, Heinemann U (1998) Altered Ca2+ signaling and mitochondrial deficiencies in hippocampal neurons of trisomy 16 mice: a model of Down's syndrome. J Neurosci 18:7216–7231

Shetty HU, Holloway HW, Acevedo LD, Galdzicki Z (1996) Brain accumulation of myo-inositol in the trisomy 16 mouse, an animal model of Down's syndrome. Biochem J 313:31–33

Shetty HU, Siarey RJ, Galdzicki Z, Stoll J, Rapoport SI (2000) Ts65Dn mouse, a Down syndrome model, exhibits elevated myo-inositol in selected brain regions and peripheral tissues. Neurochem Res 25: 431–435

Shonk T, Ross BD (1995) Role of increased cerebral myo-inositol in the dementia of Down syndrome. Magn Reson Med 33: 858–861

Sun L, June Liu S (2007) Activation of extrasynaptic NMDA receptors induces a PKC-dependent switch in AMPA receptor subtypes in mouse cerebellar stellate cells. J Physiol 583:537–553